Ab Initio and Kinetic Calculations for the Reactions of $NH(X^3\Sigma^-)$ with CH_xF_{4-x} and CD_xF_{4-x} ($x = 1, 2, 3, 4$)

Baoshan Wang,* Hua Hou, and Yueshu Gu

School of Chemistry, Shandong University, Jinan, Shandong 250100, P. R. China

Received: July 2, 1999; In Final Form: September 3, 1999

The direct hydrogen abstraction mechanisms on $^3A''$ potential surfaces for the reactions of $NH(^3\Sigma^-)$ with CH_4, CH_3F, CH_2F_2, and CHF_3 have been studied systematically using ab initio molecular orbital theory. The G2(MP2) calculations reveal that all reactions involve significant energy barriers. The effect of fluorine substitution was examined. The NH + CHF_3 reaction was found to possess the highest barrier among the four reactions. The barriers for both NH + CH_3F and NH + CH_2F_2 reactions are about 2 kcal/mol lower than that for the NH + CH_4 reaction. The rate constants for the four reactions have been deduced using transition-state theory with asymmetric Eckart tunneling correction and hindered rotor approximation over the temperature range 200−3000 K. The following least-squares-fitted expressions for the rate constants were obtained: $k^H_1(NH+CH_4) = (9.41 \times 10^{-18})T^{2.28}\ e^{-10233/T}$, $k^H_2(NH+CH_3F) = (1.69 \times 10^{-18})T^{2.31}\ e^{-9217/T}$, $k^H_3(NH+CH_2F_2) = (1.52 \times 10^{-18})T^{2.32}\ e^{-9080/T}$, $k^H_4(NH+CHF_3) = (2.12 \times 10^{-18})T^{2.29}\ e^{-10750/T}$, in $cm^3molecule^{-1}\ s^{-1}$. The deuterium kinetic isotope effects have also been investigated. All reactions show the significant and "normal" kinetic isotope effects.

I. Introduction

The NH radical is an important intermediate in combustion processes with N-containing compounds. The reactions of NH are of significance in pyrolysis and oxidation of ammonia and in industrial applications for NO_x emission reduction such as the thermal $DeNO_x$ and the $RAPRENO_x$ processes.[1,2] The reactions between NH and several highly reactive species (e.g., NO, H, O, O_2, NO_2, etc.) have been well characterized.[3−10]

The reactions of NH with hydrocarbons are of special interest because of their distinct reactivity depending on the electronic state of the NH radical.[11] The reactions of the first excited-state $NH(a^1\Delta)$ with hydrocarbons have been studied extensively.[12−15] However, the corresponding reactions of electronic ground-state $NH(X^3\Sigma^-)$ with hydrocarbons are rarely studied despite their practical and theoretical significance. The paucity of kinetic information about these reactions is due to the extreme experimental difficulty in preparing suitable laboratory conditions for reliable kinetic measurements. $NH(X^3\Sigma^-)$ is less reactive than $NH(a^1\Delta)$. Unlike the rapid reactions between $NH(X^3\Sigma^-)$ and radical species,[3−10] the slow rates of the reactions of $NH(X^3\Sigma^-)$ with hydrocarbons at room temperature require the experiments to be done at higher temperatures. However, when the temperatures are elevated, secondary reactions become competitive and, most of all, the hydrocarbons begin to decompose and form reactive species that can rapidly react with NH. Therefore, the experimental studies have been limited to the reactions of $NH(X^3\Sigma^-)$ with several carefully selected hydrocarbons (e.g., CH_4, C_2H_4, C_6H_6, etc.).[16−18] Moreover, only a rather small temperature range of about 1000−1500 K could be covered.

Fluorocarbon chemistry has importance in a variety of areas including atmospheric chemistry, combustion/flame suppression, and plasma etching in the microelectronics industry. However, because the halogenated hydrocarbons are more favorable to decompose at high temperatures than the unsubstituted hydrocarbons,[19] there is no experimental study of the reactions of $NH(X^3\Sigma^-)$ with halogenated hydrocarbons to date.

It is evident that the theoretical investigations of the reactions of $NH(X^3\Sigma^-)$ with hydrocarbons can be very meaningful. Using high-level ab initio molecular orbital theory, we not only can reveal the detailed reaction mechanism but also can predict quantitatively kinetic data from first principles over a wide temperature range. The following four reactions were found to display interesting mechanistic and kinetic behavior and thus are the subjects of this theoretical work:

$$NH(X^3\Sigma^-) + CH_4 \rightarrow NH_2 + CH_3 \qquad \Delta H = 12.4\ \text{kcal/mol} \quad (1)$$

$$NH(X^3\Sigma^-) + CH_3F \rightarrow NH_2 + CH_2F \qquad \Delta H = 8.7\ \text{kcal/mol} \quad (2)$$

$$NH(X^3\Sigma^-) + CH_2F_2 \rightarrow NH_2 + CHF_2 \qquad \Delta H = 10.2\ \text{kcal/mol} \quad (3)$$

$$NH(X^3\Sigma^-) + CHF_3 \rightarrow NH_2 + CF_3 \qquad \Delta H = 15.2\ \text{kcal/mol} \quad (4)$$

where the heats of reaction were calculated using the experimental enthalpies of formation for various species in refs 20 and 21.

Theoretically, only reaction 1 was studied previously by Fueno et al.[22] at the UHF/4-31G level. A barrier of 37.7 kcal/mol was reported. It is obvious that their study is rather rough. Several features of the present study are the following: (i) The reaction mechanisms are revealed. (ii) The potential energy surfaces are calculated at the G2(MP2) level. (iii) The rate constants are obtained over a temperature range 200−3000 K.

* Corresponding author. E-mail: guojz@icm.sdu.edu.cn.

10.1021/jp992284j CCC: $18.00
Published on Web 10/26/1999

(iv) The effect of fluorine substitution is studied. (v) The deuterium kinetic isotopic effects (KIEs) are reported. Since the corresponding reactions of the first excited-state NH($a^1\Delta$) were well studied,[12−15] more detailed kinetic data about the NH($X^3\Sigma^-$) reactions will help to understand the influence of electronic excitation in chemical reactions. Our theoretical results might be useful for further experimental measurements in the kinetic communities.

II. Qualitative Predictions

It is useful to analyze qualitatively reactions 1−4 before performing computations. NH($X^3\Sigma^-$) is the isoelectronic species of O(^{3}P) and $CH_2(X^3B_1)$. The dominant mechanisms in the reactions of O(^{3}P) and $CH_2(X^3B_1)$ with methane and fluoromethanes have been claimed to be direct hydrogen abstraction.[23−28] Therefore, one might expect hydrogen abstraction by NH($X^3\Sigma^-$) in reactions 1−4. According to the spin and orbital adiabatic correlation rules,[29] the reactants, NH($X^3\Sigma^-$) + CH_4(X^1A_1), NH($X^3\Sigma^-$) + $CH_3F(X^1A_1)$, NH($X^3\Sigma^-$) + $CH_2F_2(X^1A_1)$, and NH($X^3\Sigma^-$) + $CHF_3(^1A_1)$, give rise to a nonlinear intermediate complex (NLC) of C_s symmetry of species $^3A''$. The products, $NH_2(X^2B_1)$ + $CH_3(^2A_2'')$, $NH_2(X^2B_1)$ + $CH_2F(^2A')$, $NH_2(X^2B_1)$ + $CHF_2(^2A')$, and $NH_2(X^2B_1)$ + $CF_3(^2A_1)$, give rise to a NLC (C_s) of species $^{1,3}A'$ + $^{1,3}A''$. Thus, the reactants and the products in reactions 1−4 can correlate directly only via a $^3A''$ potential energy surface, which is different from the *dual-state* phenomena in the reactions of O(^{3}P) with methane[24−26] and fluoromethanes.[27,28]

It can be seen that all the reactions 1−4 are endothermic. The CH_3−H, CH_2F−H, CHF_2−H, and CF_3−H bond dissociation energies are as high as 104.8, 101.1, 101.4, and 106.7 kcal/mol, respectively.[30,31] Therefore, these H abstraction reactions are expected to involve high-energy barriers. Moreover, the barriers should have rather late character. As indicated by the endothermicity and the C−H bond energy, reaction 4 is predicted to possess the highest barrier.

III. Computations

Ab initio calculations were carried out using the GAUSSIAN 94 programs.[32] The geometries of reactants, transition states, and products were optimized at the UMP2(full) level[33] with the cc-pVDZ basis set.[34] It is noted that this level of theory has been successfully used to study the reactions of O(^{3}P) with fluoromethanes.[28] The vibrational frequencies were calculated at the same level of theory in order to determine the zero-point energy (ZPE, scaled by a factor of 0.95 to eliminate known systematic errors).[35] The number of imaginary frequencies (0 or 1) indicates whether a minimum or a transition state has been located. The intrinsic reaction coordinate (IRC) calculation[36] confirms that the transition state connects the designated reactants and products. Finally, the MP2 optimized geometries were utilized to obtain the total energies via the inexpensive G2(MP2) method.[37]

Because reactions 1−4 possess high energies of activation, the rate constants k can be evaluated reasonably by the nonvariational transition-state theory[38] with the tunneling correction κ using the asymmetric Eckart potential:[39]

$$k(T) = \kappa\alpha\frac{k_B T}{h}\exp\left(\frac{-\Delta G^{\ddagger}(T)}{k_B T}\right) \qquad (5)$$

where α is the statistical factor, k_B is Boltzmann's constant, h is Planck's constant, and $\Delta G^{\ddagger}(T)$ is the standard-state free energy of activation. The reliability of this procedure has been well demonstrated in the rate calculations for several analogous reactions.[40−42]

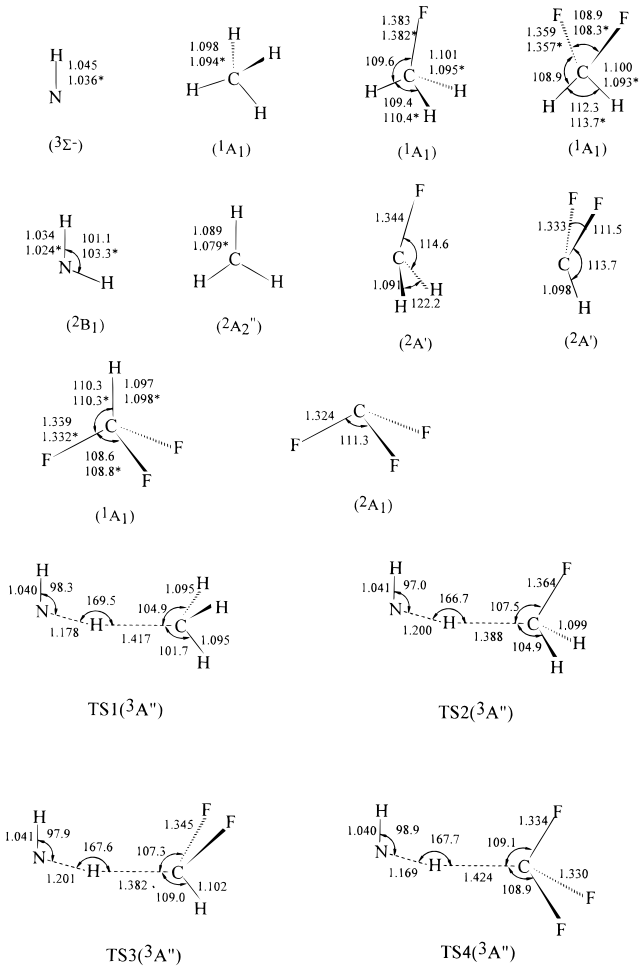

Figure 1. UMP2(full)/cc-pVDZ optimized geometries for the reactants, transition states, and products. Bond distances are in angstroms and angles are in degrees. The data with asterisks are the experimental values.

IV. Results and Discussion

The optimized geometries of the reactants, transition states, and products are shown in Figure 1. The vibrational frequencies for the reactants and the products (including those for the isotope species) are listed in Table 1. Table 2 lists the vibrational frequencies for the transition states. The heats of reaction and the energy barriers are summarized in Table 3. The comparison between the calculated rate constants and the experimental values for the NH + CH_4 reaction is depicted in Figure 2. The predicted rate constants for the reactions of NH with fluoromethanes are shown in Figure 3.

1. Reliability of the Calculations. It is worth stating the reliability of the calculations in this work. Since unrestricted Hartree−Fock (UHF) reference wave functions are not spin eigenfunctions for open-shell species, we monitored the expectation values of $\langle S^2\rangle$ in the UMP2(full)/cc-pVDZ optimization. As shown in Table 3, $\langle S^2\rangle$ was always in the range 0.762−0.754 for doublets and in the range 2.014−2.054 for triplets. After spin annihilation, the values of $\langle S^2\rangle$ are 0.75 for doublets and 2.00 for triplets, where 0.75 and 2.00 are the exact values for a pure doublet and a pure triplet, respectively. Thus, spin contamination is not severe. This suggests that a single determinant reference wave function for these systems is suitable for the level of theory used in the optimization.[43]

TABLE 1: Scaled Vibrational Frequencies (in cm^{-1}) for the Reactants and the Products in Reactions 1−4[a]

species	frequencies	exptl fundamentals[45−47]
NH	3175	3126[b]
NH_2	1492, 3247, 3349	1497, 3219, 3301
NHD	1309, 2402, 3300	
CH_3	369, 1358 (2), 3026, 3220 (2)	580, 1383 (2), 3002, 3184 (2)
CD_3	286, 999 (2), 2140, 2401 (2)	
CH_2F	676, 1135, 1145, 1427, 3040, 3193	
CD_2F	532, 870, 987, 1185, 2194, 2388	
CHF_2	526, 1012, 1135, 1163, 1311, 3036	−, −, 1164, 1173, 1317, −
CDF_2	523, 817, 911, 1117, 1222, 2238	
CH_4	1273 (3), 1490 (2), 2934, 3079 (3)	1306 (3), 1534 (2), 2917, 3019 (3)
CD_4	961 (3), 1054 (2), 2075, 2281 (3)	998 (3), 1092 (2), 2118, 2260 (3)
CH_3F	1052, 1149 (2), 1430 (2), 1434, 2938, 3038 (2)	1049, 1182 (2), 1464 (2), 1467, 2930, 3006 (2)
CD_3F	884 (2), 971, 1036 (2), 1131, 2106, 2256 (2)	
CH_2F_2	510, 1085, 1097, 1139, 1230, 1423, 1477, 2968, 3047	529, 1090, 1113, 1178, 1262, 1435, 1508, 2948, 3014
CD_2F_2	503, 885, 928, 980, 998, 1145, 1175, 2154, 2273	
CHF_3	488 (2), 672, 1100, 1148 (2), 1362 (2), 3055	507 (2), 700, 1117, 1152 (2), 1372 (2), 3036
CDF_3	509 (2), 701, 999 (2), 1125, 1276 (2), 2377	

[a] Numbers in parentheses represent degrees of degeneracy. [b] This value is taken from a very recent measurement (Ram, R. S.; Bernath, P. F.; Hinkle, K. H. *J. Chem. Phys.* **1999**, *110*, 5557).

TABLE 2: Scaled Vibrational Frequencies (in cm^{-1}) for the Transition States TS1−TS4[a]

species[a]	frequencies[b]
TS1	1771i, 67,[c] 350, 399, 570, 770, 1086, 1113, 1365, 1372, 1434, 2974, 3133, 3135, 3230
TS1	*1306i, 62,[c] 272, 293, 498, 649, 788, 904, 999, 1001, 1163, 2115, 2329, 2331, 3229*
TS2	1986i, 118,[c] 124, 379, 573, 710, 1088, 1112, 1141, 1170, 1416, 1497, 2972, 3089, 3229
TS2	*1454i, 113,[c]122, 285, 522, 636, 819, 876, 914, 984, 1123, 1190, 2150, 2304, 3228*
TS3	2062i, 50,[c] 138, 156, 506, 586, 725, 1104, 1105, 1142, 1145, 1325, 1486, 2991, 3226
TS3	*1507i, 49,[c] 138, 147, 490, 534, 662, 804, 925, 932, 1087, 1185, 1187, 2204, 3225*
TS4	1893i, 28,[c] 114, 135, 386, 488, 488, 674, 754, 1054, 1110, 1201, 1219, 1480, 3234
TS4	*1317i, 28,[c] 113, 135, 382, 484, 484, 616, 739, 770, 1079, 1197, 1206, 1212, 3233*

[a] The species in italics represent the deuterium-substituted structures. [b] The values in *italics* are the frequencies for the deuterium-substituted structures.i represents the imaginary vibrational frequency. [c] The lowest-frequency vibrations of TS1, TS2, TS3, and their deuterium transition states are considered as the internal rotations. The reduced moments of inertia are the following (in units of g mol^{-1} $Å^2$): TS1, 0.75; *TS1, 0.85*; TS2, 0.66; *TS2, 0.79*; TS3, 0.93; *TS3, 0.93*; TS4, 0.97; *TS4, 0.97*.

TABLE 3: Energy Barriers (E_a, in kcal/mol) and Heats of Reaction (ΔH, in kcal/mol) Calculated at the G2(MP2) Level for the Reactions 1−4

no.	reaction	$\langle S^2\rangle$[a]	E_a	ΔH	ΔH_{expt}[d]
1	$NH + CH_4 \rightarrow NH_2 + CH_3$	2.051	21.6	12.0	12.4
			21.6[b]	12.2[b]	
			22.3[c]	12.7[c]	
	$NH + CD_4 \rightarrow NHD + CD_3$		22.6	13.0	
2	$NH + CH_3F \rightarrow NH_2 + CH_2F$	2.054	19.6	8.9	8.7 ± 3
	$NH + CD_3F \rightarrow NHD + CD_2F$		20.6	9.8	
3	$NH + CH_2F_2 \rightarrow NH_2 + CHF_2$	2.054	19.2	9.5	10.2 ± 2
	$NH + CD_2F_2 \rightarrow NHD + CHD_2$		20.3	10.2	
4	$NH + CHF_3 \rightarrow NH_2 + CF_3$	2.054	22.1	14.5	15.2 ± 1.8
	$NH + CDF_3 \rightarrow NHD + CF_3$		23.3	15.1	

[a] The expectation values of $\langle S^2\rangle$ before projection for the transition states. For the reactants and the products, the $\langle S^2\rangle$ values are the following: NH, 2.014; NH_2, 0.758; CH_3, 0.762; CH_2F, 0.760; CHF_2, 0.756; CF_3, 0.754. [b] The G2 calculated values. [c] The G1 calculated values. [d] The experimental enthalpies of formation at 0 K from refs 20 and 21 for the reactants and products are the following (in kcal/mol): NH, 85.2; CH_4, −16.0; NH_2, 45.8; CH_3, 35.8; CH_3F, −56 ± 1; CH_2F, −7.9 ± 2; CH_2F_2, −108.2; CHF_2, −58.6 ± 2; CHF_3, −166.6 ± 0.8; CF_3, 112 ± 1.

To clarify the general reliability of the theoretical calculations, it is useful to compare the predicted chemical properties of the present particular systems of interest with experimental data. As shown in Figure 1, the geometric parameters for NH, NH_2, CH_3, CH_4, CH_3F, CH_2F_2, and CHF_3 are in good agreement with the available experimental values.[44] As can be seen from Table 1, the scaled vibrational frequencies for both the reactants and the products agree well with the experimentally observed fundamentals.[45−47] Furthermore, to check the reliability of the

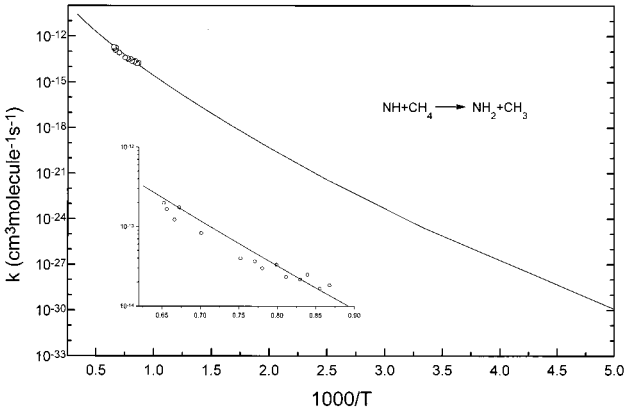

Figure 2. Plot of the logarithm of rate constants for the reactions of NH($X^3\Sigma^-$) with CH_4. For clarity, the comparison between the calculated and the experimental values in the temperature range 1150−1500 K is expanded in the insert.

calculated energetics at the G2(MP2) level, we also calculated the G1[48] and G2[49] energetics for reaction 1, which has the accurate experimental heat of reaction at 0 K.[20] As indicated in Table 3, the G2(MP2) calculated energy barrier for reaction 1 is virtually equal to the G2 value, and the heat of reaction obtained at the G2(MP2) level is in very good agreement with both the experimental values and the G1, G2 values. Additionally, the G2(MP2) heats of reaction for reactions 2−4 are also in agreement with their respective experimental values. All these good agreements provide confidence that the G2(MP2) level is adequate to calculate the energetics. The comparison of the G2(MP2) C−H bond dissociation energies (D_0) for CH_4, CH_3F,

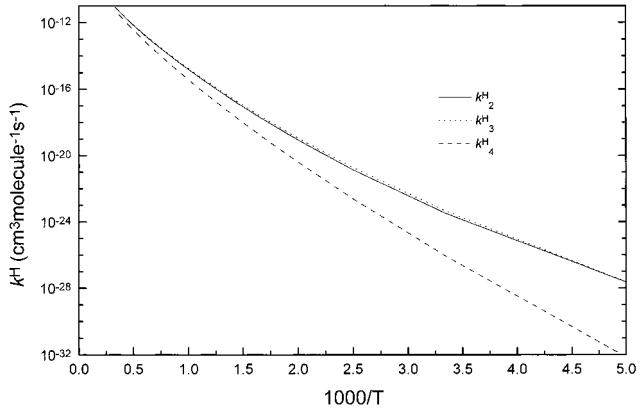

Figure 3. Plot of the logarithm of rate constants for the reactions of NH($X^3\Sigma^-$) with fluoromethanes: k^H_2, NH + $CH_3F \rightarrow NH_2 + CH_2F$; k^H_3, NH + $CH_2F_2 \rightarrow NH_2 + CHF_2$; k^H_4, NH + $CHF_3 \rightarrow NH_2 + CF_3$.

CH_2F_2, and CHF_3 to the experimental data also results in the same conclusion. The theoretically predicted values are the following (in kcal/mol): $D_0(CH_3-H) = 104.8$, $D_0(CH_2F-H) = 101.2$, $D_0(CHF_2-H) = 101.7$, and $D_0(CF_3-H) = 106.7$. The corresponding experimental values[30,31] are 104.8 ± 0.2, 101.1 ± 1.0, 101.4 ± 1.0, and 106.7 ± 1.0. Obviously, an excellent agreement is obtained.

2. Reaction Mechanism. As expected, direct hydrogen abstraction transition states, namely, TS1, TS2, TS3, and TS4 in Figure 1, are located for reactions 1, 2, 3, and 4, respectively. Each transition state has C_s symmetry and a $^3A''$ electronic state, which is consistent with that surmised from spin and orbital correlation rules. In principle, each transition state has four possible structural forms defined by two dihedral angles: τ(HNHC) and τ(NHCH) in TS1 and TS3, and τ(HNHC) and τ(NHCF) in TS2 and TS4. The four forms are (cis, trans), (cis, cis), (trans, trans), and (trans, cis). However, optimizations at the UMP2(full)/cc-pVDZ level reveal that only one structure is the true transition state, which is characterized by only one imaginary frequency. For instance, TS1 is found to be the (cis, trans) structure. The (cis, cis) structure corresponds to a second-order saddle point with two imaginary frequencies. The larger imaginary frequency is consistent with that of the (cis, trans) structure, and the smaller one actually results from the internal rotation around the breaking C···H bond. Neither (trans, trans) nor (trans, cis) structure exists because the optimization inevitably converges to the (cis, cis) and the (cis, trans) structures, respectively. Similarly, TS2, TS3, and TS4 are found to be the (cis, cis), (cis, trans), and (cis, cis) structures, respectively.

It is worth noting that the IRC calculation for reaction 1 exhibits a CH_4···NH complex on the reactant side and a CH_3···HNH complex on the product side. The corresponding H···N and C···H bond distances in the fully optimized structures are both about 2.7 Å. The analogous complexes are found in reactions 2−4. It is evident that these complexes result from the very weak long-range interactions. The binding energies are calculated to be less than 0.2 kcal/mol (including the ZPE corrections) at the UMP2(full)/cc-pVDZ level. Therefore, these shallow minima are of negligible importance in the abstraction reactions.

There are two geometric features for TS1−TS4. One is that they have the nearly collinear N···H···C structures. The angles of NHC are 169.5°, 167.6°, and 167.7°, respectively. This indicates that the hydrogen abstraction reaction prefers to occur collinearly. The other is that they are product-like structures as indicated by two aspects: (i) The breaking C−H bonds are elongated by 29%, 26%, 26%, and 30% in TS1, TS2, TS3, and TS4, respectively. (ii) The forming N−H bonds are longer than the equilibrium value in the NH_2 radical by 14%, 16%, 16%, and 13%, respectively. The HNH angles in the transition states are very close to that in the NH_2 radical. As mentioned above, the rather late character in these transition states is in accordance with the high endothermicities of the reactions 1−4. Additionally, it is interesting to note that the breaking C···H bond distances are in the order of TS4 ∼ TS1 > TS2 ∼ TS3. However, the forming N−H bond distances have the reverse order. This type of changing trend of bond distances not only reveals the effect of fluorine substitution but also reflects the sequence of energy barriers.

Table 2 shows that the hydrogen abstraction transition states have large imaginary frequencies which implies that the quantum tunneling effect may be significant and may play an important role in the reactions. It is noted that each transition state involves a very low vibrational frequency, which originates from a large-amplitude motion of the methyl (or fluoromethyl) group around the reactive bond. The low frequency indicates that at the transition state the methyl (or fluoromethyl) group has a small barrier to internal rotation.

Table 3 lists the energy barriers for reactions 1−4 calculated at the G2(MP2) level. It is obvious that all reactions possess relatively high barriers. Reaction 4 has the highest barrier of 22.1 kcal/mol at the G2(MP2) level, in accordance with its highest endothermicity and the strongest C−H bond in the CHF_3 molecule. Certainly, this barrier is only slightly higher than that for reaction 1, which involves a barrier of 21.6 kcal/mol. The barriers for reactions 2 and 3 are calculated to be 19.6 and 19.2 kcal/mol, respectively, at the G2(MP2) level.

It is worth discussing the effect of fluorine substitution on the energy barriers for the four reactions. When one of the hydrogen atoms in CH_4 is substituted by the fluorine atom, the barrier height for the corresponding reaction, i.e., reaction 2, is reduced by about 2.0 kcal/mol. This can be attributed to the weakening of the C−H bond and the decrease of the reaction endothermicity. If one of the hydrogen atoms in CH_3F is replaced by a second fluorine atom, the corresponding barrier height barely changes. It is not surprising that the reactions 2 and 3 have close energies of activation because both their endothermicities and the C−H bond strengths in CH_3F and CH_2F_2 are nearly identical. However, as mentioned above, the barrier for the NH + CHF_3 reaction becomes slightly larger than that for the NH + CH_4 reaction. This may be caused by the stabilization of trifluoromethyl, which makes the C−H bond in CHF_3 becomes somewhat stronger than that in CH_4.[31]

3. Kinetic Calculation. We have calculated the rate constants of reactions 1−4 over a wide temperature range 200−3000 K using eq 5. The vibrational frequencies, moments of inertia, and the barrier heights are taken directly from the ab initio data in this work. It should be noted that in the rate calculation the low-frequency vibration at the transition state has been treated as a hindered internal rotation using the hindered rotor (HR) model developed by Truhlar et al.[50] The partition function for the hindered rotor is approximated as

$$Q^{hin} = Q^{har} f$$

where Q^{har} is the harmonic partition function at temperature T. f is an interpolating function expressed as

$$f = \tanh(Q^{fr} u)$$

where Q^{fr} is the free rotor partition function at temperature T,

$$Q^{fr} = 0.36(I_r T)^{1/2}/\sigma_{ir}$$

and $u = h\nu/(k_B T)$. I_r is the reduced moment of inertia (in g mol^{-1} Å^{-2}) for the internal rotation, which was calculated from the geometric parameters of the transition states using Herschbach's scheme,[51] σ_{ir} is the symmetry number for the internal rotation, and ν is the frequency.

The rate constants for reaction 1 were calculated first for the purpose of comparison, and the results are depicted in Figure 2. It is encouraging that the calculated values are in quite good agreement with the experimental data in the range 1150−1500 K.[16] This agreement not only demonstrates that the G2(MP2) calculation for the reaction of NH($X^3\Sigma^-$) with CH_4 is reliable (note that the energy barrier of 37.7 kcal/mol reported by Fueno et al.[22] must be overestimated significantly) but also implies that the direct hydrogen abstraction mechanism by NH($X^3\Sigma^-$) is valid. Therefore, the calculations for the reactions of NH($X^3\Sigma^-$) with the fluoromethanes, namely, CH_3F CH_2F_2 and CHF_3, are expected to have similar accuracy. However, one should remember that the rate constants were deduced only by the conventional transition-state theory (CTST). Although all of the reactions 1−4 involve the high and distinct barriers, the theoretically predicted rate constants may be still overestimated slightly—especially at higher temperatures—because of the neglect of variational effects.

As shown in Figures 2 and 3, the rate constants k^H_1, k^H_2, k^H_3, and k^H_4 for the reactions 1, 2, 3, and 4, respectively, exhibit apparently non-Arrhenius behavior, which results from the significant tunneling effect at lower temperatures. Over the whole temperature range of interest, k^H_4 is the smallest one. k^H_2 is very close to k^H_3. At temperatures below 900 K, the rate constants for all reactions are lower than 10^{-15} cm^3 molecule^{-1} s^{-1}. It indicates that the reactions of NH($^3\Sigma^-$) with methane and fluoromethanes do proceed very slowly at lower temperatures. Both k^H_2 and k^H_3 are larger than k^H_1 at $T < 800$ K. However, with the elevation of temperatures, all the rate constants increase rapidly. Moreover, k^H_1 exceeds k^H_2 and k^H_3. At $T > 2500$ K, the rate constants are about 10^{-11} to 10^{-12} cm^3 molecule^{-1} s^{-1}. So the reactions of NH($^3\Sigma^-$) may play an important role in combustion processes. The rate constants for reactions 1−4 have been fitted to the three-parameter formula by the least-squares method as follows (in units of cm^3 molecule^{-1} s^{-1}):

$$k^H_1 = (9.41 \times 10^{-18})T^{2.28}\, e^{-10233/T}$$

$$k^H_2 = (1.69 \times 10^{-18})T^{2.31}\, e^{-9217/T}$$

$$k^H_3 = (1.52 \times 10^{-18})T^{2.32}\, e^{-9080/T}$$

$$k^H_4 = (2.12 \times 10^{-18})T^{2.29}\, e^{-10750/T}$$

4. Kinetic Isotope Effects (KIEs). We have also studied the kinetic isotope effects (KIEs) for reactions 1−4 because the KIEs can provide unique insight into the dynamics of chemical reactions.[52,53] For such direct hydrogen abstraction reactions, only the deuterium KIEs are found to be important and thus are examined in this work. The deuterium KIEs for reactions 1−4 are defined as the ratios k^H_1/k^D_1, k^H_2/k^D_2, k^H_3/k^D_3, and k^H_4/k^D_4, respectively, where k^Hs are the rate constants for the reactions of NH with the unsubstituted alkanes and k^Ds are the rate constants for those in which all protiums in alkanes are substituted by deuterium. By definition, a KIE is "normal" if it is greater than unity; otherwise, it is "inverse".[53]

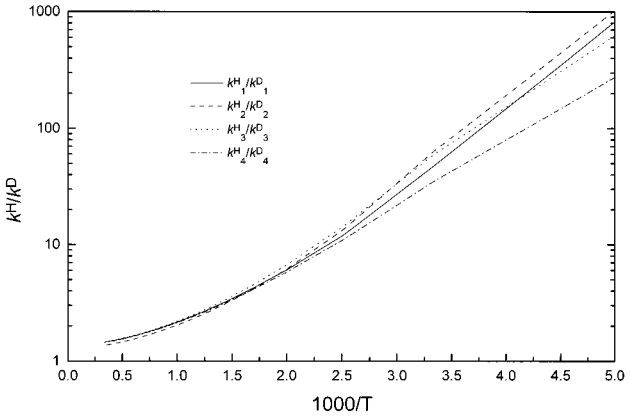

Figure 4. Deuterium KIEs for the reactions of NH($X^3\Sigma^-$) with methane and fluoromethanes vs 1000/T. See text for definition.

The D abstractions are apparently different from the H abstractions in two aspects. (i) Table 2 shows that the imaginary frequencies of the transition states are lowered by about 500 cm^{-1}. So the tunneling effect in the D abstraction reactions becomes somewhat weaker than that in the H abstraction reactions. However, the lowest vibrational frequencies show little change. (ii) As shown in Table 3, the deuterium-substituted reactions are somewhat more endothermic than the unsubstituted reactions. Furthermore, it is interesting to note that the barriers for the former also become about 1.0 kcal/mol higher than those for the latter. Therefore, the rates of the D abstractions should be slower than those of the H-abstractions. As a result, the calculated KIEs (see Figure 4) are always larger than unity over the whole temperature range of interest, especially at lower temperatures. On one hand it shows that the KIEs are "normal" for the reactions of NH($X^3\Sigma^-$) with methane and fluoromethanes; on the other hand, it indicates that the KIEs are extremely significant for all reactions. It is worth noting that the KIEs for reactions 1−4 are nearly identical above 500 K. For completeness, the rate constants k^D for the substituted reactions have also been fitted to the three-parameter expressions as follows (in units of cm^3 molecule^{-1} s^{-1}):

$$k^D_1 = (2.60 \times 10^{-17})T^{2.14}\, e^{-10994/T}$$

$$k^D_2 = (5.39 \times 10^{-18})T^{2.16}\, e^{-9996/T}$$

$$k^D_3 = (4.78 \times 10^{-18})T^{2.16}\, e^{-9879/T}$$

$$k^D_4 = (5.85 \times 10^{-18})T^{2.15}\, e^{-11505/T}$$

V. Conclusions

In this paper we have studied systematically the reactions of NH($X^3\Sigma^-$) with CH_4, CH_3F, CH_2F_2, and CHF_3 using the G2(MP2) method. Both the reaction mechanism and the rate constants for the range 200−3000 K were reported. Several major conclusions can be drawn from this calculation.

(i) The G2(MP2) level of theory is adequate for describing the potential energy surfaces for the title reactions. This is supported by the good agreement of both the calculated properties of various species and the rate constants of NH + CH_4 with the available experimental measurements.

(ii) The title reactions proceed via the direct hydrogen abstraction mechanism. The rates of the reactions are very slow because of the significant barriers involved. However, the rates increase rapidly with elevated temperatures. Meanwhile, the rate

constants show non-Arrhenius behavior resulting from significant tunneling.

(iii) The abstraction reactions occur collinearly. The transition states involved have rather late character.

(iv) The best-estimated energy barrier for the NH + CH_4 reaction is 21.6 kcal/mol. The barriers for both NH + CH_3F and NH + CH_2F_2 reactions are about 2 kcal/mol lower than that for the NH + CH_4 reaction. However, the barrier for the NH + CHF_3 reaction appears to be slightly higher than that for the NH + CH_4 reaction.

(v) The title reactions show significant and "normal" KIEs.

Supporting Information Available: Tables S1, S2, and S3 list the **Z** matrices for TS−TS4, the total energies for various species in reactions 1−4, and the values of the rate constants (k^H_1, k^H_2, k^H_3, k^H_4, k^D_1, k^D_2, k^D_3, and k^D_4), respectively, Figure S1 shows the result of the IRC calculation for the reaction of NH with CH_4. This material is available free of charge via the Internet at http://pubs.acs.org.

References and Notes

(1) Lyon, R. K. Method for Reduction of the Concentration of NO in Combustion Effluents Using Ammonia. U.S. Patent 3,900,554, 1975.

(2) Perry, R. A. NO Reduction Using Sublimation of Cyanuric Acid. U.S. Patent 4,731,231, 1988.

(3) Miller, J. A.; Bowman, C. T. *Prog. Energy Combust. Sci.* **1989**, *15*, 287.

(4) Patel-Misra, D.; Dagdigian, P. *J. Phys. Chem.* **1992**, *96*, 3232.

(5) Walch, S. P. *J. Chem. Phys.* **1993**, *98*, 1170.

(6) Durant, J. L., Jr. *J. Phys. Chem.* **1994**, *98*, 518.

(7) Bradley, K. S.; McCabe, P.; Schatz, G. C.; Walch, S. P. *J. Chem. Phys.* **1995**, *102*, 6696.

(8) Simonson, M.; Bradley, K. S.; Schatz, G. C. *Chem. Phys. Lett.* **1995**, *244*, 19.

(9) Mebel, A. M.; Morokuma, K.; Lin, M. C. *J. Chem. Phys.* **1994**, *101*, 3916.

(10) Mertens, J. D.; Chang, A. Y.; Hanson, R. K.; Bowman, C. T. *Int. J. Chem. Kinet.* **1991**, *23*, 173.

(11) Fueno, T.; Bonacic-Koutecky, V.; Koutecky, J. *J. Am. Chem. Soc.* **1983**, *105*, 5547.

(12) Tsunashima, S.; Hotta, M.; Sato, S. *Chem. Phys. Lett.* **1979**, *64*, 435.

(13) Kajimoto, O.; Fueno, T. *Chem. Phys. Lett.* **1981**, *80*, 484.

(14) Freitag, F.; Rohrer, F.; Stuhl, F. *J. Phys. Chem.* **1989**, *93*, 3170.

(15) Hack, W.; Rathmann, K. *Ber. Bunsen-Ges. Phys. Chem.* **1990**, *94*, 1304.

(16) Rohig, M.; Wagner, H. Gg. *Ber. Bunsen-Ges. Phys. Chem.* **1994**, *98*, 858.

(17) Rohig, M.; Wagner, H. Gg. *Ber. Bunsen-Ges. Phys. Chem.* **1994**, *98*, 864.

(18) Rohig, M.; Roemming, K.; Wagner, H. Gg. *Ber. Bunsen-Ges. Phys. Chem.* **1995**, *99*, 105.

(19) Schug, K. P.; Wagner, H. Gg.; Zabel, F. *Ber. Bunsen-Ges. Phys. Chem.* **1979**, *83*, 167.

(20) Curtiss, L. A.; Raghavachari, K.; Redfern, P. C.; Pople, J. A. *J. Chem. Phys.* **1997**, *106*, 1063.

(21) DeMore, W. B.; Sander, S. P.; Golden, D. M.; Hampson, R. F.; Kurylo, M. J.; Howard, C. J.; Ravishankara, A. R.; Kolb, C. E.; Molina, M. J. *Chemical Kinetics and Photochemical Data for Use in Stratospheric Modeling*; JPL Publication 97-4; Jet Propulsion Laboratory: Pasadena, CA, 1997.

(22) Fueno, T.; Kajimoto, O.; Koutecky, V. B. *J. Am. Chem. Soc.* **1984**, *106*, 4062.

(23) Boehland, T.; Dobe, S.; Temps, F.; Wagner, H. Gg. *Ber. Bunsen-Ges. Phys. Chem.* **1985**, *89*, 1110.

(24) Gonzalez, C.; McDouall, J. J. W.; Schlegel, H. B. *J. Phys. Chem.* **1990**, *94*, 7467.

(25) Walch, S. P.; Dunning, T. H., Jr. *J. Chem. Phys.* **1980**, *72*, 3221.

(26) Schatz, G. C.; Wagner, A. F.; Dunning, T. H., Jr. *J. Phys. Chem.* **1984**, *88*, 221.

(27) Kreye, W. C. *Chem. Phys. Lett.* **1996**, *256*, 383.

(28) Wang, B.; Hou, H.; Gu, Y. *Chem. Phys.* **1999**, *247*, 201.

(29) Shuler, K. E. *J. Chem. Phys.* **1953**, *21*, 624.

(30) Baldwin, R. R.; Drewery, G. R.; Walker, R. W. *J. Chem. Soc., Faraday Trans. 1* **1984**, *80*, 2827.

(31) Leroy, G.; Sana, M.; Wilante, C.; Nemba, R. M. *J. Mol. Struct.* **1989**, *198*, 159.

(32) Frisch, M. J.; Trucks, G. W.; Schlegel, H. B.; Gill, P. W. M.; Johnson, B. G.; Robb, M. A.; Cheeseman, J. R.; Keith, T. A.; Petersson, G. A.; Montgomery, J. A.; Raghavachari, K.; Allaham, M. A.; Zakrzewski, V. G.; Ortiz, J. V.; Foresman, J. B.; Cioslowski, J.; Stefanov, B. B.; Nanayakkara, A.; Challacombe, M.; Peng, C. Y.; Ayala, P. Y.; Chen, W.; Wong, M. W.; Andres, J. L.; Replogle, E. S.; Gomperts, R.; Martin, R. L.; Fox, D. J.; Binkley, J. S.; Defrees, D. J.; Baker, J.; Stewart, J. P.; Head-Gordon, M.; Gonzales, C.; Pople, J. A. *Gaussian 94*, revision E.1; Gaussian Inc.: Pittsburgh, PA, 1995.

(33) Møller, C.; Plesset, M. S. *Phys. Rev.* **1934**, *46*, 618.

(34) Woon, D. E.; Dunning, T. H., Jr. *J. Chem. Phys.* **1993**, *98*, 1358.

(35) Hehre, W.; Radom, L.; Schleyer, R. V. R.; Pople, J. A. *Ab Initio Molecular Orbital Theory*; Wiley: New York, 1986.

(36) Gonzalez, C.; Schlegel, H. B. *J. Chem. Phys.* **1989**, *90*, 2154.

(37) Curtiss, L. A.; Raghavachari, K.; Pople, J. A. *J. Chem. Phys.* **1993**, *98*, 1293.

(38) Laidler, K. J. *Chemical Kinetics*, 3rd ed.; Harper and Row: New York, 1987.

(39) Johnston, H. S.; Heicklen, J. *J. Chem. Phys.* **1962**, *66*, 533.

(40) Corchado, J. C.; Espinosa-Garcia, J.; Hu, W.-P.; Rossi, I.; Truhlar, D. G. *J. Phys. Chem.* **1995**, *99*, 687.

(41) Yu, Y.; Li, S.; Xu, Z.; Li, Z.; Sun, C. *Chem. Phys. Lett.* **1998**, *296*, 131.

(42) Mebel, A. M.; Lin, M. C. *J. Phys. Chem. A* **1999**, *103*, 2088.

(43) Liu, R.; Francisco, J. S. *J. Phys. Chem. A* **1998**, *102*, 9869.

(44) Lide, D. R. *CRC Handbook of Chemistry and Physics*; CRC Press: Boca Raton, FL, 1992; Vol. 73, p 9.

(45) Jacox, M. E. *J. Phys. Chem. Ref. Data* **1984**, *13*, 945.

(46) Mizuno, M.; Saeck, S. *Spectrochim. Acta A* **1976**, *32*, 1077.

(47) Zachariah, M. R.; Westmoreland, P. R.; Burgess, D. R., Jr.; Tsang, W.; Melius, C. F. *J. Phys. Chem.* **1996**, *100*, 8737.

(48) Pople, J. A.; Head-Gordon, M.; Fox, D. J.; Raghavachari, K.; Curtiss, L. A. *J. Chem. Phys.* **1989**, *90*, 5622.

(49) Curtiss, L. A.; Raghavachari, K.; Trucks, G. W.; Pople, J. A. *J. Chem. Phys.* **1991**, *94*, 7221.

(50) Truhlar, D. G. *J. Comput. Chem.* **1991**, *12*, 266.

(51) Herschbach, D. R.; Johnston, H. S.; Pitzer, K. S.; Powell, R. E. *J. Chem. Phys.* **1956**, *25*, 736.

(52) Lu, D.-h.; Maurice, D.; Truhlar, D. G. *J. Am. Chem. Soc.* **1990**, *112*, 6206.

(53) Melissas, V. S.; Truhlar, D. G. *J. Chem. Phys.* **1993**, *99*, 3542.